Formation of liquid crystalline phase of actin filament solutions and its dependence on filament length as studied by optical birefringence

Atsushi Suzuki,* Tadakazu Maeda,‡ and Tadanao Ito*

*Department of Biophysics, Faculty of Science, Kyoto University, Kyoto 606; and ‡Mitsubishi Kasei Institute of Life Sciences, Machida, Tokyo 194, Japan

ABSTRACT We studied the formation and structure of liquid crystalline phase of F-actin solutions by polarized light photometry, assuming that a small domain of the liquid crystalline phase works as a linear retardation plate. Transmittance of polarized light due to the birefringence of liquid crystalline phase appeared above a threshold concentration of F-actin. The threshold increased with a decrease in filament length, which was regulated by calcium-activated gelsolin. The intensity increased linearly with increasing concentrations until it reached a stationary value. The deviation of optical axis direction of the putative retardation plate was estimated 7–15 degrees. These results indicate that: (*a*) the liquid crystalline phase is formed above a threshold concentration of F-actin; (*b*) the threshold is proportional to the inverse of filament length; (c) the ordered phase coexists with the isotropic one, increasing the volume fraction with increasing concentrations until all filaments take the liquid crystalline structure; (*d*) the filaments in liquid crystalline phase take a highly ordered array.

These results can be attributed to the excluded volume effect of rod-like molecules on the formation of liquid crystalline structure.

INTRODUCTION

Actin filament (F-actin) takes various forms in cytoplasm of nonmuscle cell, for example, a crystalline-like tight bundle in intestine microvilli, a liquid crystalline-like loose bundle in stress fiber of fibroblast, an isotropic gel-like structure in macrophage cytoplasmic cortex and so forth (Stossel, 1984). These individual structures are indispensable for specific biological functions in which F-actin participates.

There are many actin-binding proteins that interact specifically with F-actin and bring about the crystalline-like tight bundle, or liquid crystalline-like loose bundle in vitro (Stossel et al., 1985). Interestingly, F-actin itself can form a crystalline-like tight bundle in the absence of actin binding proteins at high concentrations of divalent cations, low pH (Kawamura and Maruyama, 1970; Hanson, 1973), or in the presence of macromolecules (Suzuki et al., 1989). These results indicate that the tight bundle structure observed in vivo might be thermodynamically stable. On the other hand, little is known about liquid crystalline formation of F-actin, although such formation of a rod-like biopolymer was predicted theoretically (Onsager, 1949; Ishihara, 1951; Flory, 1956) and also demonstrated experimentally in other biopolymers, such as synthetic polypeptide or DNA (Miller et al., 1974; Strezelecka et al., 1988).

Address correspondence to Dr. Tadanao Ito, Department of Biophysics, Faculty of Science, Kyoto University, Kyoto, 606, Japan, Fax: 81-75-791-0271.

Here we report on our analysis of optical birefringence of F-actin solution that demonstrates that a highly ordered liquid crystalline structure is formed at concentrations of F-actin above a threshold. The experimental results quantitatively agree with theoretical analysis based on the excluded volume effect of rod-like molecules (Onsager, 1949; Ishihara, 1951; Flory, 1956).

MATERIALS AND METHODS

Monomeric actin (G-actin) was prepared from rabbit skeletal muscle according to Spudich and Watt (1971). Gelsolin was prepared from swine serum according to Doi et al. (1987) with slight modification. Briefly, 30–60% ammonium sulfate fraction of the serum was passed through Q-Sepharose (Pharmacia Fine Chemicals, Piscataway, NJ) and DEAE-Sephadex A-50 columns (Pharmacia Fine Chemicals), and the active peak was further purified by passage of hydroxyapatite (Bio-Rad Laboratories, Richmond, CA) and Blue-Sepharose 6B (Pharmacia Fine Chemicals) columns. The G-actin and gelsolin concentrations were estimated using extinction coefficients, E_M^{290} of 2.66×10^4 and E_M^{280} of 1.18×10^5, respectively (Yin et al., 1988). G-actin was polymerized into filamentous form (F-actin) in F-buffer (100 mM KCl, 2 mM $MgCl_2$, 0.2 mM $CaCl_2$, 0.2 mM ATP, 10 mM imidazole-HCl, pH 7.5). For the sample of the optical birefringence measurement, G-actin was added to F-buffer in the cuvette at ice-cold temperature, and then the polymerization was started by raising the temperature to room temperature. To regulate filament length, G-actin was polymerized in the presence of gelsolin and the average length was determined from actin/gelsolin ratio, *r*, which was assumed to equal the number of actin monomers/filament (Janmey et al., 1986).

A Carl Zeiss, Inc. (Thornwood, NY) universal-type microscope equipped with a pair of crossed polarizers was used as the polarized light microscope. The polarizer was set on the lamp field iris and the

0006-3495/91/01/25/06 $2.00

analyzer was inserted into the fixed position behind the objective. A Hitachi spectrophotometer U-3200 was used to measure transmittance in the polarized light photometry system shown in Fig. 2.

RESULTS

Liquid crystalline phase detected by a polarized microscope

Fig. 1 shows photographs of F-actin solutions under a polarized microscope. There was no birefringence at 1.8 mg/ml of F-actin (*a*). A remarkably high birefringence could be observed at higher concentrations and the degree of the birefringence increased with increasing concentrations (*b*, *c*). Characteristic striped patterns often appeared locally (*d*), and the contrast of the pattern in the same objective field was reversed by rotating the microscope stage (*e*, *f*). This indicates that there are ordered domains that have optical axes of different directions, and each of them preferentially orients parallel to the glass-liquid interface in the microscope sample. From these results it is concluded that F-actin solutions separate spontaneously into an isotropic phase and an anisotropic, ordered one above 2 mg/ml and the anisotropic phase should correspond to a liquid crystalline phase.

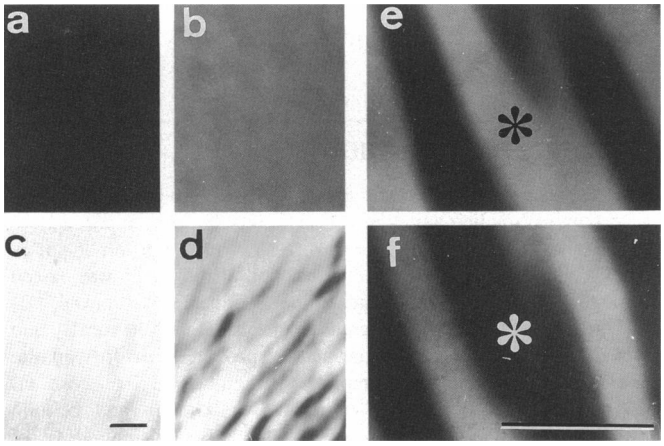

FIGURE 1 Photographs of F-actin solutions under a polarized microscope. Concentrations of F-actin are: 1.8 mg/ml (*a*), 4.5 mg/ml (*b*), and 6.3 mg/ml (*c*, *d*). *a*, *b*, and *c* correspond to the main areas of the individual samples, and *d* to the local area in which the characteristic striped patterns were observed. *e* and *f* represent the striped patterns observed at 5.4 mg/ml and the asterisk (*) denotes the same objective field, whose brightness was reversed by rotating the microscope stage. G-actin was polymerized in F-buffer (100 mM KCl, 2 mM $MgCl_2$, 0.2 mM $CaCl_2$, 0.2 mM ATP, 10 mM imidazole-HCl, pH 7.5) on the slide glass. The height of the microscope sample was ~100 μm. Magnifications: ×120 in *a–d*; ×480 in *e* and *f*. Scale bars, 40 μm.

Analysis of liquid crystalline phase by a polarized light photometry; theory

Using the polarized light photometry system shown in Fig. 2, the formation of liquid crystalline phase can be quantified. We shall assume for the analysis that (*a*) F-actin solution in a cuvette is divided into small domains of equal cross-sectional areas and each of these domains corresponds to either an isotropic (Fig. 2 *b*, *shaded circles*) or an anisotropic phase (*white circles with arrow*), (*b*) the domain of the anisotropic phase works as a small linear retardation plate, the principal axis of which is parallel to the glass-liquid interface in the cuvette, and (*c*) the directions of the principal axes vary locally but the retardation Δ of each domain is constant over the cuvette. When the cuvette is placed between crossed polarizers, the transmittance I_{θ_i} through one of the small retardation plate i can be calculated using the Jones matrix (Shurcliff, 1962; see Appendix for detail).

$$I_{\theta_i} = \tfrac{1}{4} \cdot (1 - \cos \Delta) \cdot [1 - \cos 4(\theta_i - \alpha)],$$

where θ_i is the direction angle of the principle axis of the retardation plate i, and α is that of the polarization of incident light, both of which are measured counterclockwise from the *x*-axis in *x-z* plane parallel to the cuvette surface (Fig. 2). The total transmittance, *I*, through the cuvette, which is the sum of the transmittance through

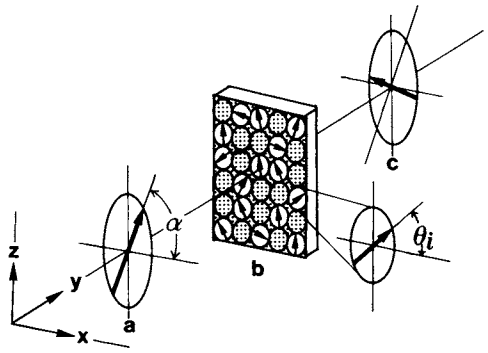

FIGURE 2 Schematic representation of the polarized light photometry system for birefringence measurement of F-actin solution. A cuvette containing F-actin solution (*b*) is placed between a pair of crossed polarizers (*a*, *c*). *x–z* plane is determined as parallel to the cuvette surface, *y* parallel to the light path. α in *a* denotes the direction of the transmission axis of the polarizer. The white circles marked on the cuvette (*b*) correspond to the putative retardation plates, where the direction of the principal axis of each retardation plate is pointed by the arrow. θ_i represents one of the direction angles of the retardation plates. The wavelength of the measurement light and the thickness of the cuvette are 450 nm and 2 mm, respectively.

each domain, and its average, $\langle I \rangle$, can be represented as:

$$I = \sum_i S_i I_{\theta_i}$$
$$= \tfrac{1}{4} \cdot (1 - \cos \Delta) \cdot \sum_i S_i [1 - \cos 4(\theta_i - \alpha)]$$
$$= \langle I \rangle - \tfrac{1}{4} \cdot (1 - \cos \Delta) \cdot \sum_i S_i \cdot \cos 4(\theta_i - \alpha), \quad (1)$$

where

$$\langle I \rangle = (2/\pi) \int_0^{\pi/2} I \, d\alpha$$
$$= \tfrac{1}{4} \cdot (1 - \cos \Delta) \cdot S \cdot \phi \propto \phi \quad (2)$$

and S is the cross-sectional area of the incident light, S_i the total area of the anisotropic ordered domains which have the same direction angle of θ_i, and ϕ the volume fraction of the ordered phase, which is defined as $\phi = \sum_i S_i/S$.

Eqs. 1 and 2 show that the total transmittance, I, has a sine-like character as a function of α, and the average value $\langle I \rangle$ is proportional to the volume fraction of the ordered domain, ϕ.

Putting Eq. 2 in the place of the first term of Eq. 1, we get

$$I = [(1 - \cos \Delta)/4] \cdot [\phi S - \sum_i S_i \cos 4(\theta_i - \alpha)].$$

Here we shall assume a Gaussian distribution on the orientation angle of the retardation plates around an average angle $\langle \theta \rangle$. We represent a deviation angle of the retardation plate from $\langle \theta \rangle$ as θ'_j, and the total area of the retardation plates having a deviation angle of θ'_j, as S_j. Because the retardation plates distribute symmetrically around $\langle \theta \rangle$, $S_j = S_k$ if $\theta'_j = -\theta'_k$. In this case, the total transmittance, I, can be represented as:

$$I = [(1 - \cos \Delta)/4] \cdot [\phi S - \sum_j S_j \cos 4(\theta'_j + \langle \theta \rangle - \alpha)]$$
$$= [(1 - \cos \Delta)/4] \cdot [\phi S - \sum_j S_j \cos 4\theta'_j \cdot \cos 4(\langle \theta \rangle - \alpha)]$$
$$= [(1 - \cos \Delta)/4]$$
$$\cdot [\phi S - \int_{-\pi/2}^{\pi/2} S(\theta') \cos 4\theta' \, d\theta' \cdot \cos 4(\langle \theta \rangle - \alpha)]$$
$$= [(1 - \cos \Delta)/4]$$
$$\cdot [\phi S - \phi S (1/\sigma\sqrt{2\pi}) \int_{-\pi/2}^{\pi/2} \exp(-\theta'^2/2\sigma^2)$$
$$\cdot \cos 4\theta' \, d\theta' \cdot \cos 4(\langle \theta \rangle - \alpha)]$$
$$\simeq \langle I \rangle [1 - \exp(-8\sigma^2) \cdot \cos 4(\langle \theta \rangle - \alpha)] \quad (3)$$

since

$$\sum_j S_j \sin 4\theta'_j = 0$$
$$S(\theta') = \left(\sum_j S_j\right) \cdot (1/\sigma\sqrt{2\pi}) \exp(-\theta'^2/2\sigma^2)$$
$$= \phi S \cdot (1/\sigma\sqrt{2\pi}) \exp(-\theta'^2/2\sigma^2),$$

where $S(\theta')$ is the total area of the retardation plates having a deviation angle of θ' and σ is the standard deviation of the Gaussian distribution. The error attributed to the above approximation of the definite integral is $<0.01\%$, if $\sigma < 0.5$. The approximation should hold well in the present study because all the σ values estimated from the experimental data were <0.4.

Eq. 3 shows that the amplitude of the total transmittance, I, depends on the distribution of θ_i. Consequently, measuring the transmittance, I, as a function of α enables us to estimate the volume fraction of liquid crystalline phase and also the degree of the array of the putative retardation plates.

Analysis of liquid crystalline phase by polarized light photometry; experiments

As predicted by Eq. 3, the total transmittance, I, as a function of α showed experimentally a sine-like character, although its phase was not always indentical. The time course of I for 6.8 mg/ml F-actin solution is plotted in Fig. 3, where the phase of each function is set the same for simplicity. Transmittance increased gradually after polymerization. The experimental curves fit quite well to the theoretical prediction (see Eq. 3), in which

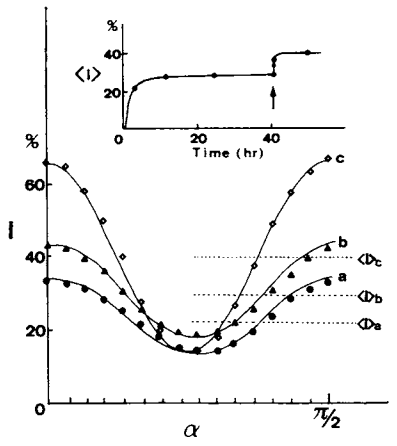

FIGURE 3 Time course of transmittance, I, of F-actin solution after polymerization. G-actin (6.8 mg/ml) was polymerized in the cuvette containing F-buffer. After allowing the solution to stand for an appropriate time at room temperature, the transmittance, I, was measured as a function of α with or without adding gentle agitation by a couple of upside-down inversions. (●): 3 h without agitation; (▲): 13 h without agitation; (◇): 48 h with agitation. The solid lines denoted by *a*, *b*, *c*, respectively, represent the theoretical curves derived from Eq. 3, setting σ as 0.30 for *a*, 0.32 for *b*, and 0.22 for *c*. $\langle I \rangle_a$, $\langle I \rangle_b$, and $\langle I \rangle_c$ are the average values of *a*, *b*, and *c*, respectively. The inset shows the time course of $\langle I \rangle$ after polymerization. At the time pointed by the arrow, the sample was gently agitated by a couple of upside-down inversions.

the values of standard deviation σ are set as 0.30 for the data of 3 h after polymerization (*a*), 0.32 of 13 h (*b*), and 0.22 of upside-down inversions (*c*), respectively. The value obtained by upside-down inversions indicates that ~70% of the putative retardation plates have optical axes aligned within 13 degrees.

The average value of transmittance, $\langle I \rangle$, also increased gradually when the F-actin solutions were allowed to stand without agitation, but it arrived at a stationary value immediately after gently agitating the solutions with upside-down inversions (Fig. 3, *inset*). The value was unchanged for more than 1 d and further inversions of the cuvette did not increase it. These results indicate that the agitation should simply accelerate the kinetics by which the liquid crystalline arrays form, and give a rationale for determining the stationary value of $\langle I \rangle$ after gentle agitation.

The stationary value of $\langle I \rangle$ increased linearly with increasing concentrations of F-actin from 2.0–6.5 mg/ml, above which $\langle I \rangle$ was almost independent of the concentration (Fig. 4, *open circles*). The results indicate that the liquid crystalline phase appears at a threshold concentration, 2.0 mg/ml in this case, and it coexists with the isotropic phase until 6.5 mg/ml. The volume fraction of liquid crystalline phase increases linearly with the increase in concentration over this range (see Eq. 1); above 6.5 mg/ml the solution is uniformly in a liquid crystalline phase.

Effects of the filament length on the formation of liquid crystalline phase

The stationary values of $\langle I \rangle$ of F-actin solutions polymerized at various actin/gelsolin molar ratios (*r*) are plotted in Fig. 4 as functions of actin concentration. Formation of the liquid crystalline phase strongly depended on *r*, indicating that shorter filament forms it at higher concentrations. The F-actin polymerized at $r = 350$ did not take the liquid crystalline phase at concentrations below 9 mg/ml. The threshold concentrations are plotted as a function of the inverse of *r* in Fig. 5. The upper abscissa represents the inverse of the average filament length, *L*, calculated from *r* using the equation $L = (r/370)$ μm (Janmey et al., 1986; Hanson and Lowry, 1963).

When F-actin filament in the liquid crystalline phase was severed by gelsolin, which was activated by the addition of micromolar order of calcium ion, *I* values of the solution gradually decreased (Fig. 6). This means that conversion of the liquid crystalline phase to the isotropic one occurred spontaneously by shortening of F-actin to a length that could not form the liquid crystalline phase.

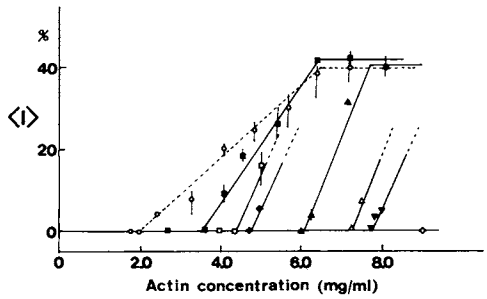

FIGURE 4 Average values of the stationary transmittance $\langle I \rangle$ as a function of F-actin concentrations. After polymerizing G-actin in the cuvette containing F-buffer for 1 h in the absence or presence of gelsolin at various molar ratios to G-actin, the solution was gently agitated with a couple of upside-down inversions, and was allowed to stand for 30 min at room temperature before the transmittance was measured. (○): F-actin polymerized in the absence of gelsolin; (■): *r* (actin/gelsolin) = 1,200; (□): $r = 1{,}000$; (◆): $r = 850$, (▲): $r = 700$, (△): $r = 600$; (▼): $r = 530$, (◇): $r = 350$.

DISCUSSION

An actin filament can be regarded rheologically as a stiff rod (Zaner and Stossel, 1983; Janmey et al., 1986). Theoretical analysis predicts that a liquid crystalline phase appears in a solution of hard rod molecules above a threshold concentration even in the absence of an attractive interaction. This is thought to be due to the parallel array of the rod molecules which decreases the excluded volume (Onsager, 1949; Ishihara, 1951; Flory, 1956).

Assuming that the domain of the liquid crystalline phase would work as a linear retardation plate, our analysis of the optical birefringence given by the liquid crystalline structure showed that the liquid crystalline

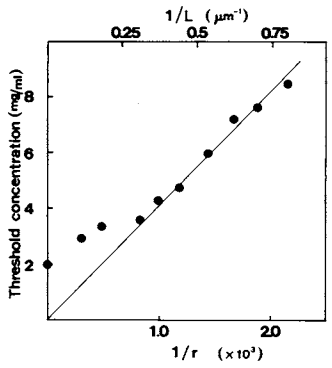

FIGURE 5 The threshold concentrations of liquid crystalline formation as a function of the inverse of actin/gelsolin ratio, *r*. The upper abscissa represents the inverse of the average filament length, *L*, calculated by the equation $L = (r/370)$ μm.

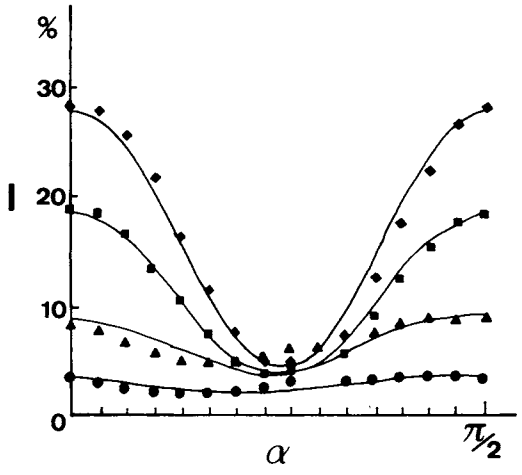

FIGURE 6 Time course of disappearance of the transmittance, *I*, caused by calcium-activated gelsolin. G-actin (5.4 mg/ml) was polymerized in calcium-omitted F-buffer (100 mM KCl, 2 mM $MgCl_2$, 1 mM $CaCl_2$, 0.2 mM ATP, 10 mM imidazole-HCl, pH 7.5) for 1 h in the presence of gelsolin at the molar ratio of actin/gelsolin = 350:1, and allowed to stand for 30 min after a couple of upside-down inversions. Then an aliquot of calcium solution was added to make the final concentration of 1 mM. After the addition of calcium, the sample solution was allowed to stand without agitation for an appropriate time and the transmittance was measured as a function of α. (◆): 30 min; (■): 270 min; (▲): 14.6 h; (●): 20 h.

phase of F-actin solution appeared above a threshold concentration. It coexisted at first with the isotropic phase and increased its fraction with increasing concentrations, as predicted theoretically (Fig. 4). Our results from the time course of the formation of the liquid crystalline phase and the effect of mild shear forces indicate that the transition of the isotropic structure to the liquid crystalline one should be a diffusion-limited process and the gentle shear forces facilitate the process by aligning the direction of the filaments.

Our results (Fig. 4) also indicate that the threshold concentration is strongly dependent on filament length; shorter filaments required a higher concentration of F-actin. Inverse proportionality of threshold concentration to filament length has been obtained theoretically by Onsager (1949) and Flory (1956). If V_c is taken as the volume fraction at the threshold concentration and X as the axial ratio of the filament, the relation $V_c = K/X$ holds ($K = 3.3$ by Onsager, $K = 8$ by Flory). In the present experiments, the threshold concentration increased proportionally to the inverse of actin/gelsolin ratio, r, smaller than 2000:1 (Fig. 5). We calculated the average filament length using r, because the powerful nucleation activity of gelsolin makes the average number of actin monomers/filament equal to r (Janmey et al., 1986). The results indicate that the expected inverse proportionality holds between the threshold concentration and the average filament length shorter than 3 μm. If we take the diameter of F-actin as 7 nm, we obtain a K value of 10, which agrees with the theoretical one. The deviation from inverse proportionality at low gelsolin content might be due to the uncertainty of the average length estimated from the actin/gelsolin ratio (Janmey et al., 1986).

The standard deviation of optical axes of the putative retardation plates, σ, was small and almost independent of whether the sample was agitated with the upside-down inversions or not. For example, in the case of F-actin polymerized without gelsolin, the observed values were 0.25–0.3 at 4.5 mg/ml (nonagitated), 0.22 at 6.8 mg/ml (agitated), and 0.12 at 7.7 mg/ml (nonagitated), respectively. The estimated distribution angle of the optical axis should be <7–15 degrees. A highly ordered array of the optical axis should result from an ordered arrangement of actin filaments in the liquid crystalline phase. In fact, Flory (1956) states that the distribution angle of the direction of hard rod molecule with an axial ratio of 50–200 should be 10.2–11.0 degrees in the liquid crystalline phase.

Each domain of liquid crystalline phase observed under the microscope was considerably large, and its optical axis oriented parallel to the glass-liquid interface preferentially (Fig. 1). This may be explained as follows. Actin filaments are known to be entangled with each other at a high concentration, such as used in the present experiments (Zaner and Stossel, 1983; Doi and Edwards, 1978). In such solutions, if one or more filaments happen to array their axes parallel to the adjacent ones, the other filaments should, like falling dominos, turn toward the same direction over an extended distance. In this sense, the formation of the liquid crystalline structure might be considered "a nucleation promoted" reaction. The steric hindrance of the rotational diffusion of the filament at the glass-liquid interface should make a parallel array of the filaments much easier. Consequently, the liquid crystalline phase with the optical axis parallel to the interface should be formed predominantly.

Liquid crystalline-like structures of actin filaments can be observed in the I-band of striated muscle, in the stress fiber of nonmuscle cell, etc. The present results show that F-actin can form the liquid crystalline structure spontaneously at concentrations comparable to those in vivo. They indicate that the liquid crystalline-like structure in cytoplasm should be thermodynamically stable, although the interaction of a specific actin-binding protein with the filament brings about such an assembly structure. In addition, the formation of liquid crystalline structure in vivo might proceed in a cooperative manner, being subject to regulation by "nucleation,"

as well as by the change of filament length, as observed in vitro (Fig. 6).

APPENDIX

The transmittance through a linear retardation plate

We shall consider a linear retardation plate, the retardation, and the orientation angle of the principal axis of which are Δ and θ_i, respectively (see Fig. 2 in the text). The Jones matrix R_{Δ,θ_i} of this retardation plate can be written as (Shurcliff, 1962):

$$R_{\Delta,\theta_i} = I_{\theta_i} \cdot R_{\Delta,0} \cdot I_{-\theta_i},$$

where

$$R_{\Delta,0} = \begin{pmatrix} \exp(i\Delta/2) & 0 \\ 0 & \exp(-i\Delta/2) \end{pmatrix}$$

$$I_{\theta_i} = \begin{pmatrix} \cos\theta_i & -\sin\theta_i \\ \sin\theta_i & \cos\theta_i \end{pmatrix}.$$

Here we shall assume that the incident linearly polarized light has a direction angle of polarization of $\alpha = 0$. After polarized light has entered the retardation plate and passed through the vertical linear polarizer, the electric field vector of the light, E_{θ_i}, and the intensity of the transmittance, I_{θ_i}, are:

$$\begin{aligned} E_{\theta_i} &= \begin{pmatrix} 0 & 0 \\ 0 & 1 \end{pmatrix} \cdot R_{\Delta,\theta_i} \cdot \begin{pmatrix} 1 \\ 0 \end{pmatrix} \\ &= \begin{pmatrix} 0 \\ [\exp(i\Delta/2) - \exp(-i\Delta/2)] \sin\theta_i \cos\theta_i \end{pmatrix} \\ I_{\theta_i} &= E^*_{\theta_i} \cdot E_{\theta_i} \\ &= \tfrac{1}{4} \cdot (1 - \cos\Delta)(1 - \cos 4\theta_i). \end{aligned}$$

If the direction angle of polarization of the incident light is α, in general,

$$I_{\theta_i} = \tfrac{1}{4} \cdot (1 - \cos\Delta)\,[1 - \cos 4(\theta_i - \alpha)].$$

We thank Professor Shun-ichi Ohnishi for constant encouragement during this work.

This work was supported by a Grant-in-Aid for Scientific Research from the Ministry of Education, Japan.

Received for publication 8 June 1990 and in final form 31 August 1990.

REFERENCES

Doi, M., and S. F. Edwards. 1978. Dynamics of rod-like molecules in concentrated solution. *J. Chem. Soc. Faraday Trans. II.* 74:560–570.

Doi, Y., M. Higashida, and S. Kido. 1987. Plasma-gelsolin-binding sites on the actin sequence. *Eur. J. Biochem.* 164:89–94.

Flory, P. J. 1956. Phase equilibria in solutions of rod-like particles. *Proc. Roy. Soc. Lond. A.* 234:73–89.

Hanson, J. 1973. Evidence from electron microscope studies on actin paracrystals concerning the origin of the cross-striation in the thin filaments of vertebrate skeletal muscle. *Proc. Roy. Soc. Lond. B. Biol. Sci.* 183:39–58.

Hanson, J., and J. Lowry. 1963. The structure of F-actin and of actin filaments isolated from muscle. *J. Mol. Biol.* 6:46–60.

Ishihara, A. 1951. Theory of anisotropic colloidal solutions. *J. Chem. Phys.* 13:1142–1147.

Janmey, P. A., J. Peetermans, K. S. Zaner, T. P. Stossel, and T. Tanaka. 1986. Structure and mobility of actin filaments as measured by quasielastic light scattering, viscometry, and electron microscopy. *J. Biol. Chem.* 261:8357–8362.

Kawamura, M., and K. Maruyama. 1970. Polymorphisms of F-actin. *J. Biochem. (Tokyo).* 68:885–899.

Miller, W. G., C. C. Wu, E. L. Wee, G. L. Santee, F. H. Rai, and K. G. Goebel. 1974. Thermodynamics and dynamics of polypeptide liquid crystals. *Pure Appl. Chem.* 38:37–58.

Onsager, L. 1949. The effects of shape on the interaction of colloidal particles. *Annu. Rev. Biochem.* 51:627–659.

Shurcliff, W. A. 1962. Polarized Light. Harvard Univ. Press, Cambridge, MA.

Spudich, J. A., and S. J. Watt. 1971. The regulation of rabbit skeletal muscle contraction. *J. Biol. Chem.* 246:4866–4871.

Stossel, T. P. 1984. Contribution of actin to the structure of cytoplasmic matrix. *J. Cell Biol.* 99:15s–19s.

Stossel, T. P., C. Chaponnier, R. M. Ezzell, J. H. Hartwig, P. A. Janmey, D. J. Kwiatkowski, S. E. Lind, D. B. Smith, F. S. Southwick, H. L. Yin, and K. S. Zaner. 1985. Nonmuscle actin-binding proteins. *Annu. Rev. Cell. Biol.* 1:353–402.

Strezelecka T. E., M. W. Davidson, and R. L. Rill. 1988. Multiple liquid crystal phases of DNA at high concentrations. *Nature (Lond.).* 331:457–460.

Suzuki, A., M. Yamazaki, and T. Ito. 1989. Osmoelastic coupling in biological structures: formation of parallel bundles of actin filaments in a crystalline-like structure caused by osmotic stress. *Biochemistry.* 28:6513–6518.

Yin, H. L., K. Iida, and P. A. Janmey. 1988. Identification of a polyphosphoinositide-modulated domain in gelsolin which binds to the sides of actin filaments. *J. Cell. Biol.* 106:805–812.

Zaner, K. S., and T. P. Stossel. 1983. Physical basis of the rheological properties of F-actin. *J. Biol. Chem.* 258:11004–11009.